Supporting Information

Exploring Brannerite-type $Mg_{1-x}M_xV_2O_6$ (M = Mn, Cu, Co, or Ni) Oxides: Structure and Optical Properties

Table S1. The measured $L^*a^*b^*$ color coordinates of $Mg_{1-x}Mn_xV_2O_6$.

	L*	***a****	***b****
$x = 0.0$	54.52	12.26	43.08
$x = 0.1$	34.79	11.55	16.24
$x = 0.3$	32.20	6.78	9.62
$x = 0.5$	30.64	5.00	9.52
$x = 0.7$	28.56	2.05	1.63
$x = 0.9$	23.37	1.04	0.23
$x = 1.0$	27.44	1.67	3.78

Table S2. The measured $L^*a^*b^*$ color coordinates of $Mg_{1-x}Co_xV_2O_6$.

	L*	***a****	***b****
$x = 0.0$	54.52	12.26	43.08
$x = 0.2$	34.14	13.42	17.72
$x = 0.4$	37.23	16.93	16.87
$x = 0.6$	32.48	13.62	8.75
$x = 0.8$	23.92	0.67	2.80
$x = 1.0$	37.06	0.07	−0.73

Table S3. The measured $L^*a^*b^*$ color coordinates of $Mg_{1-x}Ni_xV_2O_6$.

	*L**	*a**	*b**
$x = 0.0$	54.52	12.26	43.08
$x = 0.1$	47.47	12.81	28.44
$x = 0.3$	39.26	17.83	23.2
$x = 0.5$	32.84	20.23	16.87
$x = 0.7$	30.74	16.61	9.75
$x = 0.9$	28.01	12.10	6.66
$x = 1.0$	24.82	9.78	3.75

Figure S1

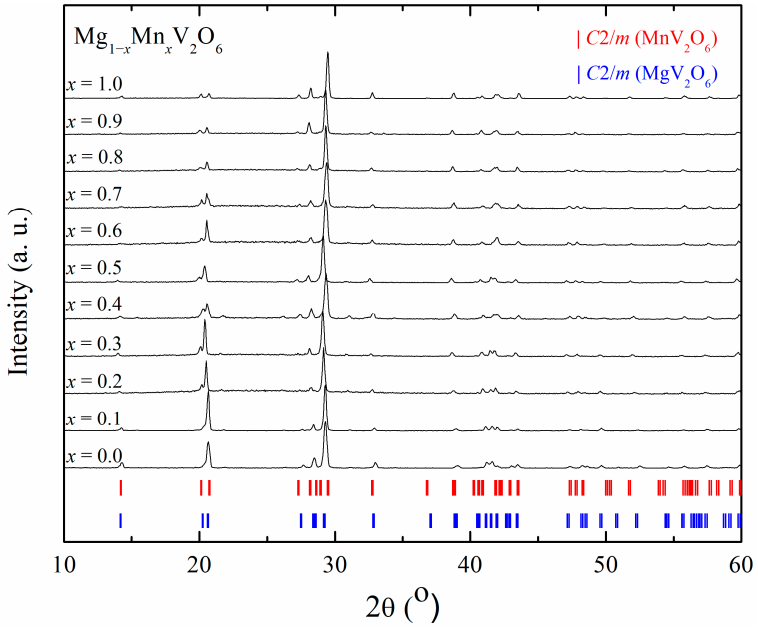

Figure S1. Powder XRD patterns of $Mg_{1-x}Mn_xV_2O_6$ (x = 0.0 - 1.0) samples that were prepared at 700 °C in air.

Figure S2

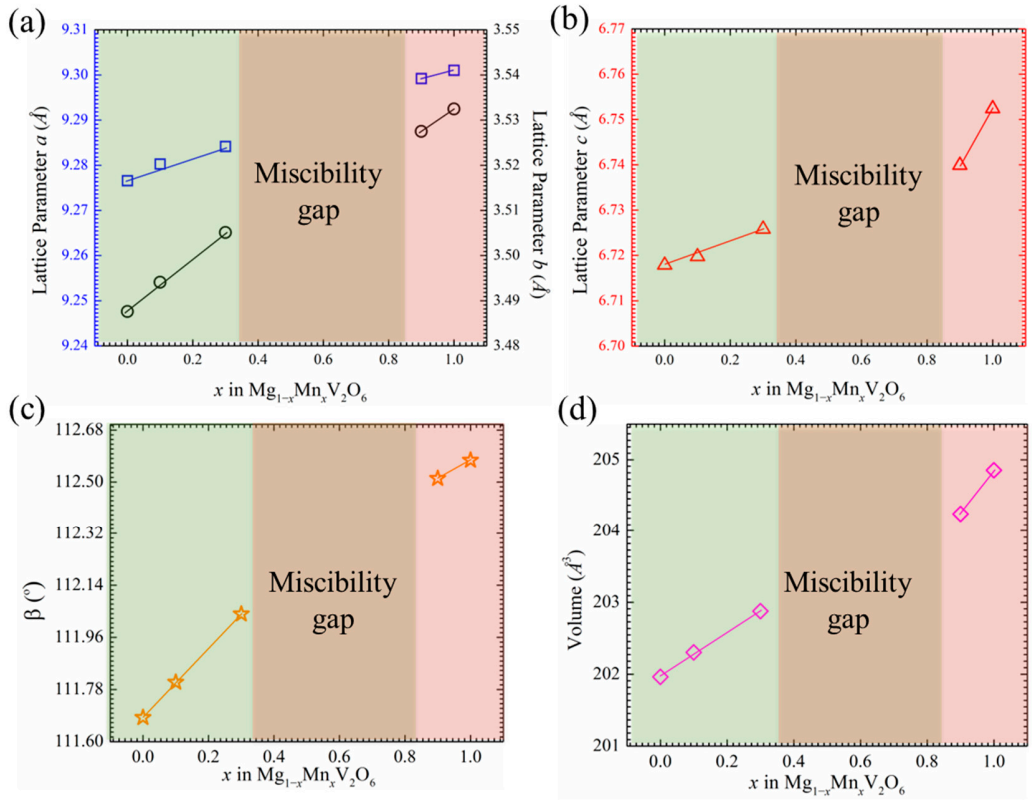

Figure S2. Variations in the (a) lattice parameters '*a*' and '*b*', (b) lattice parameter '*c*', (c) angle *β*, and (d) volume of the $Mg_{1-x}Mn_xV_2O_6$ series as a function of *x*.

Figure S3

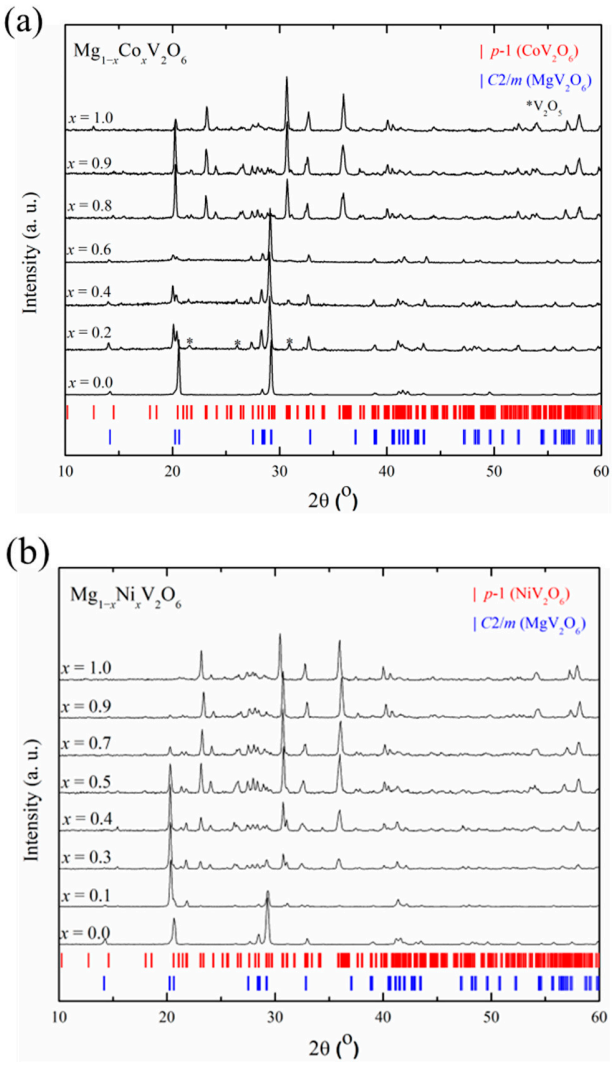

Figure S3. Powder XRD patterns of (a) $Mg_{1-x}Co_xV_2O_6$ and (b) $Mg_{1-x}Ni_xV_2O_6$ prepared at 650 °C in air.

Figure S4

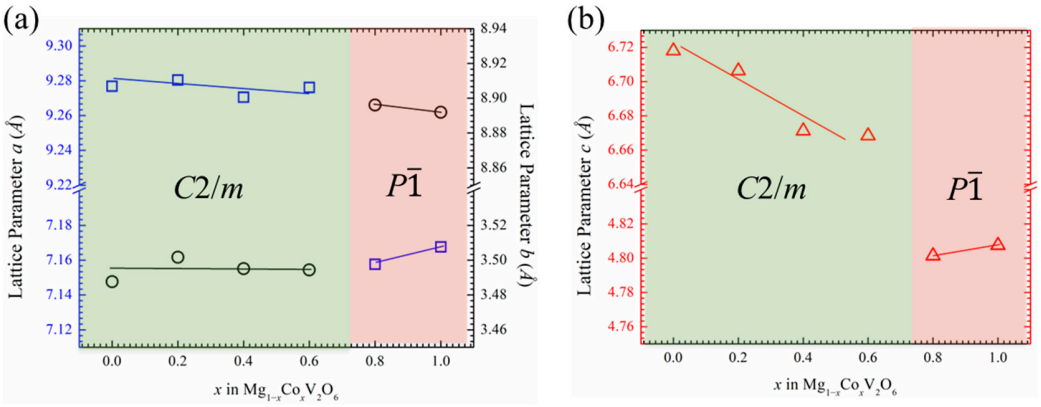

Figure S4. Variations in the (a) lattice parameters '*a*' and '*b*' and (b) lattice parameter '*c*' of the $Mg_{1-x}Co_xV_2O_6$ series as a function of *x*.

Figure S5

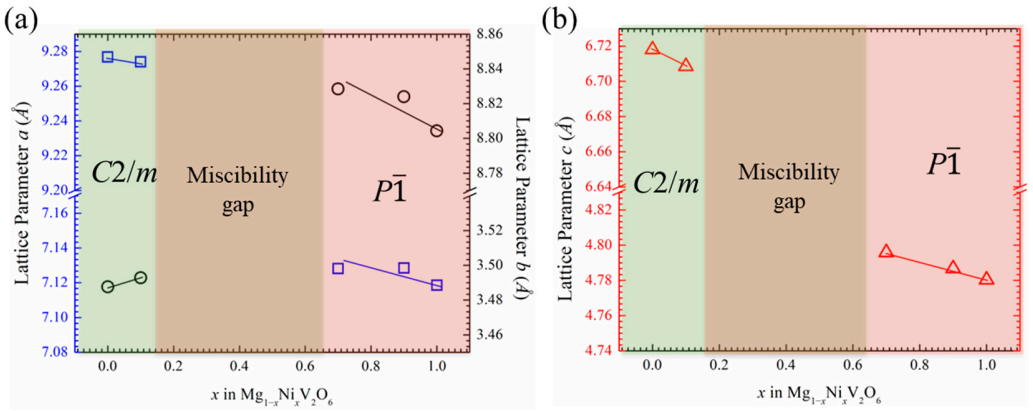

Figure S5. Variations in the (a) lattice parameters '*a*' and '*b*' and (b) lattice parameter '*c*' of the $Mg_{1-x}Ni_xV_2O_6$ series as a function of *x*.

Figure S6

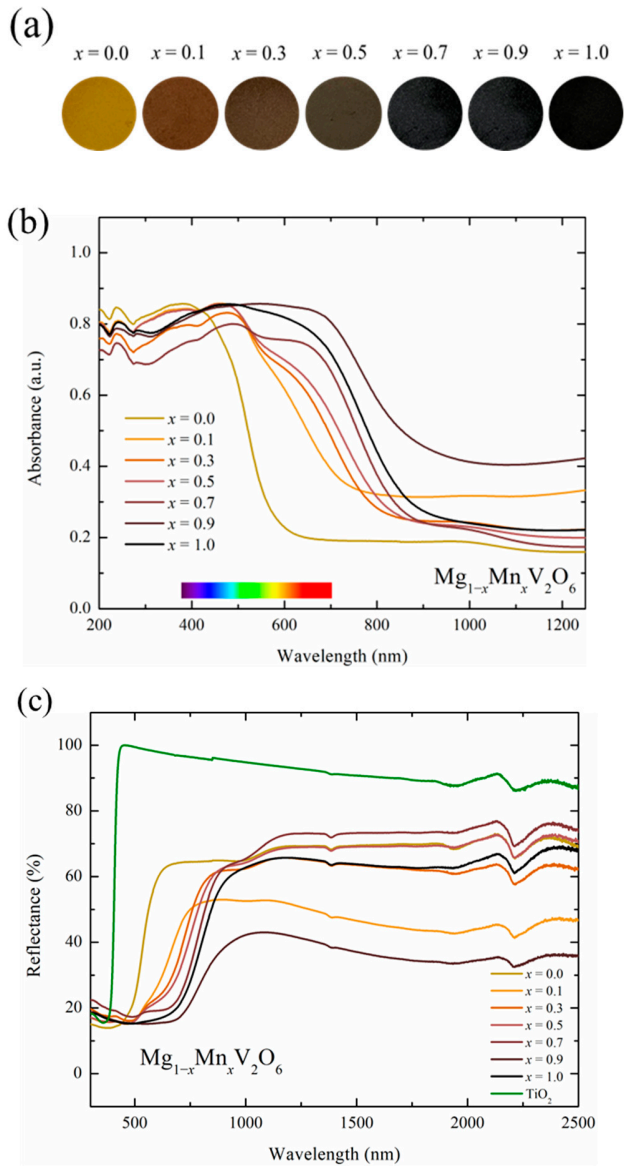

Figure S6. (a) Photographs, (b) DRUV–Vis absorbance, and (c) NIR reflectance spectra of the $Mg_{1-x}Mn_xV_2O_6$ solid solution series. The NIR reflectance of TiO_2 is also shown for comparison in (c).

Figure S7

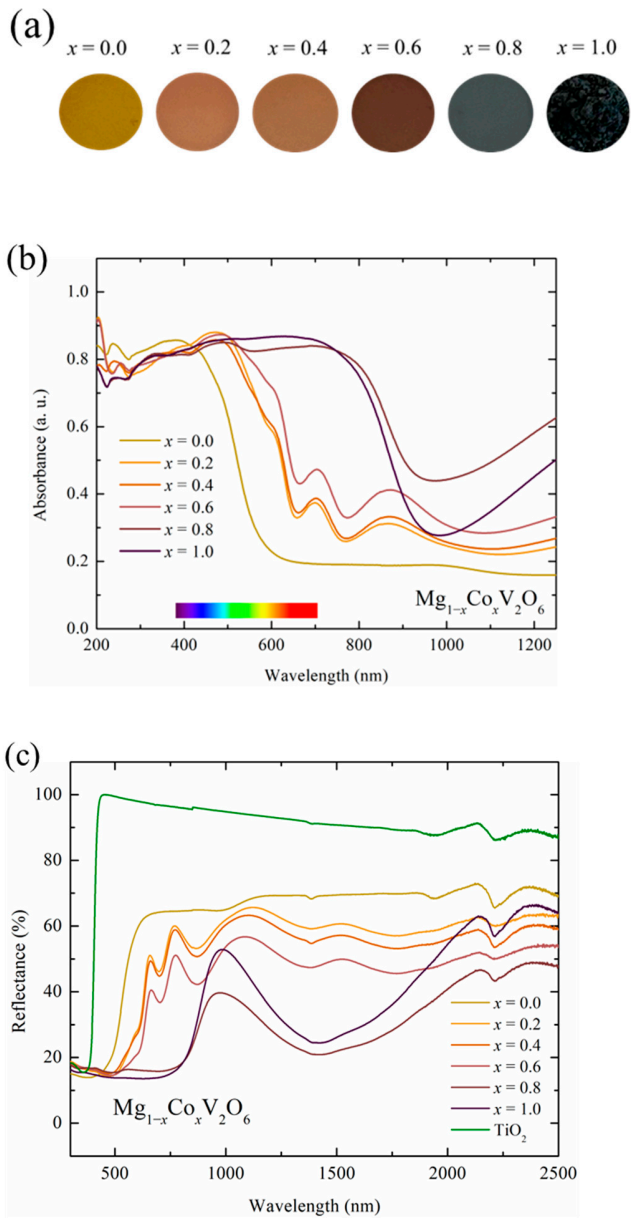

Figure S7. (a) Photographs, (b) DRUV–Vis absorbance, and (c) NIR reflectance spectra of the $Mg_{1-x}Co_xV_2O_6$ compounds, along with TiO_2.

Figure S8

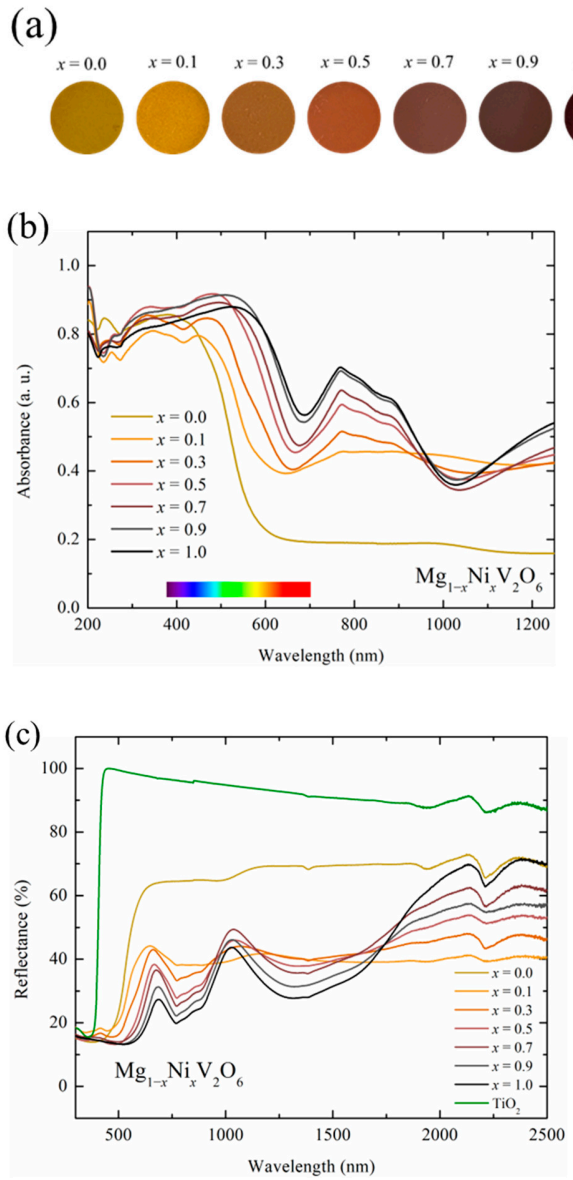

Figure S8. (a) Photographs, (b) DRUV–Vis absorbance, and (c) NIR reflectance spectra of the $Mg_{1-x}Ni_xV_2O_6$ compounds, along with TiO_2.

Figure S9

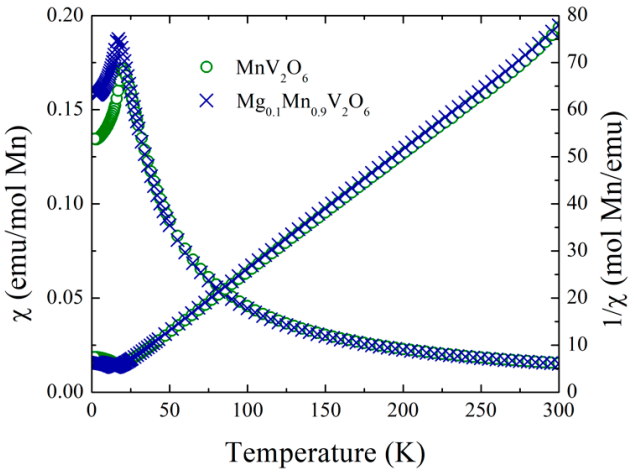

Figure S9. Magnetic susceptibility and inverse molar susceptibility vs. the temperatures of MnV_2O_6 and $Mg_{0.1}Mn_{0.9}V_2O_6$.

Figure S10

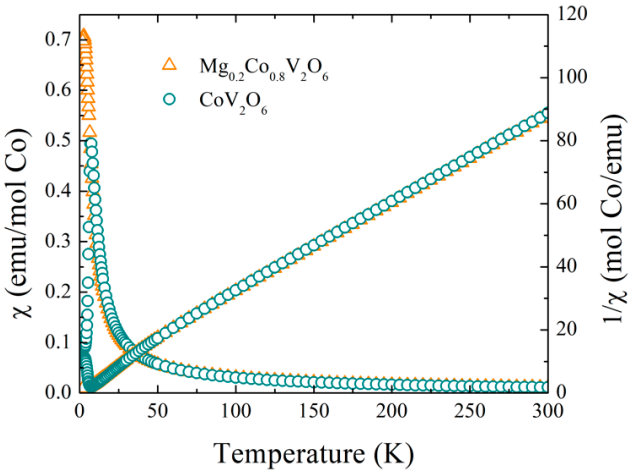

Figure S10. Magnetic susceptibility and inverse molar susceptibility vs. the temperatures of CoV_2O_6 and $Mg_{0.2}Co_{0.8}V_2O_6$.

Figure S11

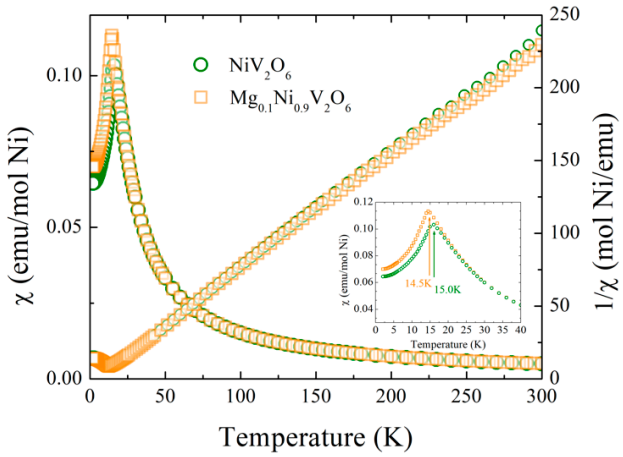

Figure S11. Magnetic susceptibility and inverse molar susceptibility vs. the temperatures of NiV_2O_6 and $Mg_{0.1}Ni_{0.9}V_2O_6$.